Acta metall. mater. Vol. 41, No. 5, pp. 1551–1557, 1993
Printed in Great Britain.

0956-7151/93 $6.00 + 0.00

A THEORY FOR CLEAVAGE CRACKING IN THE PRESENCE OF PLASTIC FLOW

Z. SUO,[1] C. F. SHIH[2] and A. G. VARIAS[2]

[1]Department of Mechanical and Environmental Engineering, University of California, Santa Barbara, CA 93106 and [2]Division of Engineering, Brown University, Providence, RI 02912, U.S.A.

(Received 9 September 1992)

Abstract—A theory is proposed for cleavage cracking surrounded by pre-existing dislocations. Dislocations are assumed not to emit from the crack front. It is argued that the pre-existing dislocations, except for occasional interceptions with the crack front, are unlikely to blunt the major portion of the crack front, so that the crack front remains nanoscopically sharp, advancing by atomic decohesion. The fracture process therefore consists of two elements: atomic decohesion and background dislocation motion. An elastic cell, of size comparable to dislocation spacing or dislocation cell size, is postulated to surround the crack tip. This near-tip elasticity accommodates a large stress gradient, matching the nanoscopic, high cohesive strength to the macroscopic, low yield strength. Consequences of this theory are explored in the context of slow cleavage cracking, stress-assisted corrosion, fast running crack, fatigue crack growth, constraint effects, and mixed mode fracture along metal/ceramic interfaces. Computational models and experiments to ascertain the range of validity of this theory are proposed.

1. INTRODUCTION

The fundamental process for plastic flow is discrete, consisting of at least two length scales: the Burgers vector $b \sim 10^{-10}$ m, and dislocation spacing $D \sim 10^{-6}$ m. On one scale, atoms exhibit individuality ultimately governed by quantum mechanics. On the other scale, dislocations interact through elasticity. Continuum plasticity applies when stress variation over a multiple of D is small compared to the macroscopic yield strength. The discreteness becomes important for events occurring between lengths b and D. In the emerging field of nanomechanics, various concepts have been proposed to bridge the two scales. The underlying assumption is that the individual atom motion gives way to the cooperative motion of many atoms, forming nanoscopic shear-bands, decohesion zones, etc. Recent mechanics studies of this kind include dislocation emission from a crack tip [1], experimental imaging of dislocation cores near nanoscopic stress concentrators [2], and dislocation cell formation [3, 4].

We explore the implications of the existence of the length scale D in a particular context: cleavage in the presence of pre-existing dislocations. It is known that a sharp, cleaving crack can propagate, slowly or dynamically, surrounded by substantial dislocation motion. For example, a sharp crack can grow slowly by cleavage along a gold/sapphire interface even though the gold deforms plastically; the measured fracture energy is much larger than the adhesive energy [5]. Similar behavior happens in copper/glass [6], copper/sapphire [7], niobium/alumina [8], and copper bicrystals contaminated by bismuth [9].

This phenomenon cannot be explained by existing mechanistic theories. Atomic cohesive strength, σ_B, is known to be orders of magnitude higher than macroscopic yield strength, σ_Y. When σ_B/σ_Y exceeds about 4, crack-bridging models within the framework of continuum plasticity predict that the crack blunts, limiting the near-tip stress to several times σ_Y [10–13]. Consequently, cleavage cannot proceed from the crack tip. Instead, one has to appeal to other fracture mechanisms, such as hole growth [14] and cleavage from a remote defect [15], both leading to rough fracture surfaces not observed in experiments cited in the previous paragraph.

A cleavable, rate-sensitive material has a low fracture resistance at high crack speeds, dislocations being outrun by the crack. A model has been developed on the basis of this picture [16, 17]. It is found that within a continuum visco-plastic formulation for a propagating crack, a square root singularity is retained, provided that the material is sufficiently rate-sensitive. This limits the model to high speed cleavage, or low dislocation mobility, which is too restrictive to account for the above experiments. It is clear that neither strong rate-sensitivity nor high crack speed can be general requirements for cleavage.

Figure 1 conveys the essentials of the present theory. Consider materials and testing conditions such that no dislocation emits from the crack tip before the crack grows. This happens, for example, for cleavable materials such as steel and silicon below the ductile–brittle transition temperature, or contaminated grain boundaries, or interfaces subjected to environmental degradation, or interfaces with a few atomic layers of brittle reaction com-

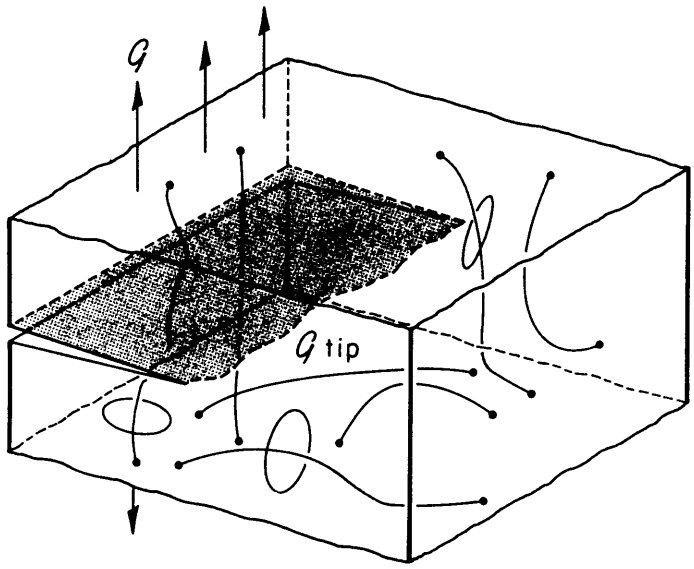

Fig. 1. A decohesion front in a network of pre-existing dislocations. The diameter of the decohesion core is about 1 nm; the average dislocation spacing is more than 100 nm.

pounds. Obviously, the competition between atomic decohesion and dislocation emission [1, 18] cannot be addressed by the present theory; instead, the consequences of the premise that dislocations do not emit from the crack front is explored in this paper. Included are slow cleavage cracking, stress-assisted corrosion, fast-running crack, fatigue cracking, constraint effects, and mixed mode fracture along metal/ceramic interfaces.

2. CLEAVAGE IN THE PRESENCE OF A DISLOCATION NETWORK

The theory is based on a single premise: the crack front does not emit dislocations. As illustrated in Fig. 1, so long as dislocation spacing D is much larger than the lattice constant, the probability for a pre-existing dislocation to blunt a major portion of the crack front should be extremely small. Consequently, a crack which does not emit dislocation will remain nanoscopically-sharp, advancing by atomic decohesion. Within the cell essentially free of dislocations which surrounds the crack front, the crystal is linearly elastic down to a nanometer. Near the crack tip, nonlinearity arises from partial atomic separation and nanoscopic shear bands. The size of the elastic cell, represented by D, is several orders of magnitude larger than the nonlinear zone size. Consequently, information regarding the nanoscopic nonlinearity is transmitted—to an observer outside the elastic cell—through a single quantity: the Griffith energy Γ_G. The elastic cell provides a medium through which the stress decays rapidly, matching the high atomic debond stress on one side, and the low macroscopic yield stress on the other. For example, with $b = 10^{-10}$ m and $D = 10^{-6}$ m, the stress decays approximately by a factor $\sqrt{(D/b)} = 100$ over a distance of 1 μm. The dislocation motion at the characteristic distance D away from the crack tip dissipates plastic energy, Γ_P, which is typically much larger than Γ_G. In summary, atoms around a crack front can be divided into three regions: nanoscopic decohesion zone, microscopic elastic cell, and macroscopic dislocation dissipative background.

The elastic cell is a nanomechanics concept with imprecise, if any, continuum description. The concept can be approximately understood in terms of spatially varying yield strengths. Sketched in Fig. 2 is yield strength varying with the distance from a representative atom at the crack tip. The theoretical shear strength is approached near the crack tip; the strength decays to the macroscopic yield strength in the

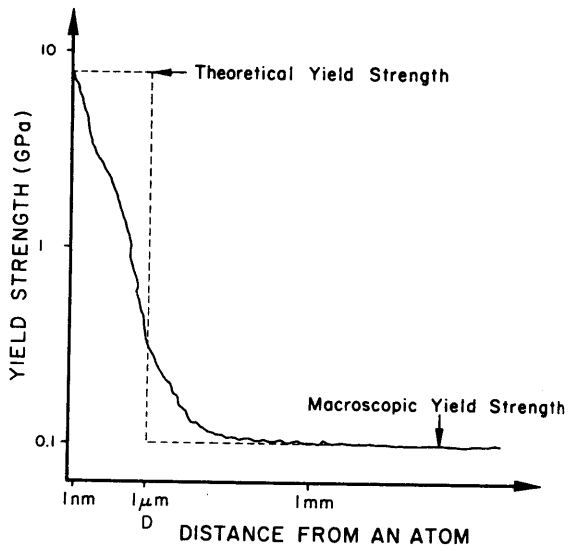

Fig. 2. Yield strength as a function of the distance from an atom at the center of an elastic cell.

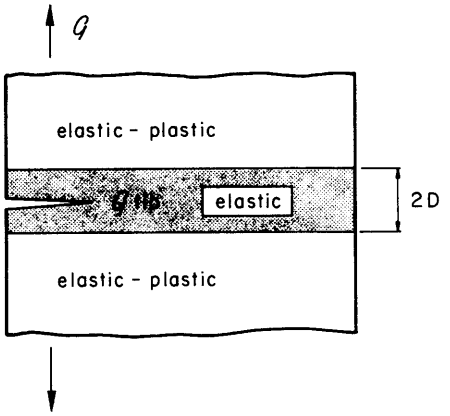

Fig. 3. A model system with a step-function decay in yield strength.

background. The shape of the decay function has not been investigated; dislocation cell models may provide some insight [3, 4]. Nevertheless, the decay function *must* have a characteristic length comparable to the dislocation spacing D.

Consider a cleavable, rate-independent material with Griffith energy Γ_G, yield strength σ_Y and yield strain $\epsilon_Y = \sigma_Y/E$, E being Young's modulus. The crack tip energy release rate, $\mathcal{G}_{tip}$, is shielded by background dislocation motion from the remotely applied energy release rate, $\mathcal{G}$. Dimensional analysis dictates that

$$\mathcal{G}/\mathcal{G}_{tip} = g(D\epsilon_Y\sigma_Y/\mathcal{G}_{tip}). \tag{1}$$

The shielding ratio g also depends on crack increment and material constants such as ϵ_Y, Poisson's ratio ν and in particular, the shape of the decay function in Fig. 2. For properties representative of metals (e.g. $D \sim 1\,\mu m$, $\epsilon_Y \sim 10^{-3}$, $\sigma_Y \sim 10^8\,N/m^2$, $\Gamma_G \sim 1\,J/m^2$), the parameter $D\epsilon_Y\sigma_Y/\Gamma_G$ ranges from 10^{-2} to 10. The parameter can be understood in several ways; e.g. all else being fixed, an increase in elastic cell size D reduces the total energy dissipation.

Under steady-state growth, $\mathcal{G}_{tip} = \Gamma_G$ and $\mathcal{G}$ equals the measured fracture energy Γ. The plastic dissipation Γ_P is given by $\Gamma = \Gamma_P + \Gamma_G$. Since typically $\Gamma_P \gg \Gamma_G$, it is sometimes assumed that Γ_G is an irrelevant parameter for fracture involving substantial plasticity. However, various authors have pointed out that if cleavage is the basic fracture mechanism, Γ_P must depend on Γ_G—that is, the small quantity Γ_G serves as a "valve" for large dissipation Γ_P (e.g. [19, 20]). In the present context, the extent of plastic zone is set by Γ_G. Similar behavior happens in transformation-toughened ceramics, where the matrix toughness sets the extent of the transformation zone and thereby the steady state toughness [21, 22].

In the present theory, it is assumed that no low strength, long range bridges, such as tearing caused by cleavage plane reorientation between neighboring grains, operate in the crack wake. These bridges are responsible for the large "cleavage energy" reported for polycrystalline steels. When operating, the bridges may serve as a bigger valve than atomic decohesion. If this is the case, a bridging law may be used in the present model. Indeed, when $\sigma_B/\sigma_Y < 4$, the present model should reduce to regular bridging model without an elastic cell [10–13].

3. SLOW CLEAVAGE CRACK GROWTH

Further simplifications are needed to make quantitative predictions (Fig. 3). The decohesion zone is small compared to D so that the square root singular elasticity solution prevails in $b \ll r \ll D$. Detailed atomistic description of decohesion is unnecessary except for a prescription of a cleavage energy Γ_G. The shape of the elastic cell is unimportant since the plastic zone height is typically much larger than D; we use a strip to represent the elastic cell. A disc translating with the crack tip can be another convenient choice, but the difference is expected to be minor in so far as $\mathcal{G}/\mathcal{G}_{tip}$ is concerned. The background dislocation motion is represented by continuum plasticity. A refinement, if needed, may include individual dislocations or a dislocation network in the transition region between the elastic cell and the continuum plastic flow.

The crack starts to grow when $\mathcal{G} \geqslant \Gamma_G$; more load is required to maintain the growth, leading to a resistance curve (R-curve, see Fig. 4). The plastic zone also increases as the crack grows, attaining a steady-state height H. The energy release rate reaches a steady-state value Γ_{SS}. The model geometry is analyzed in the steady-state using finite elements. Figure 5 shows that the shielding ratio increases rapidly as D or σ_Y decrease. The influence of strain hardening exponent, N, can also be seen. For non-hardening metals, the plastic dissipation completely shields the crack tip at a finite $D\epsilon_Y\sigma_Y/\mathcal{G}_{tip}$. In practice, D may be used as a fitting parameter to correlate experimental data. For example, a metal with $\sigma_Y = 10^8\,M/m^2$, $\epsilon_Y = 10^{-3}$ and $\Gamma_G = 1\,J/m^2$ gives

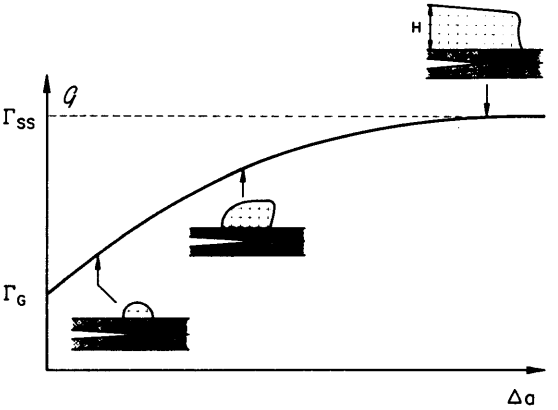

Fig. 4. A fracture resistance curve: the fracture energy increases as the crack grows.

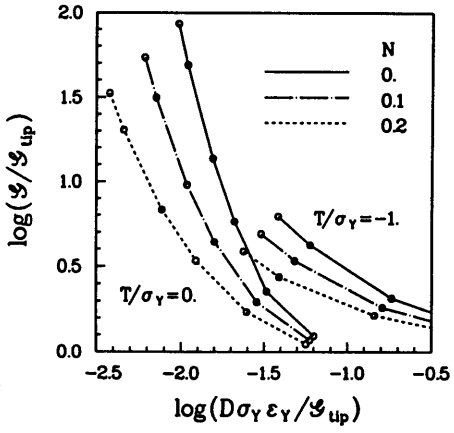

Fig. 5. Computed shielding ratio as a function of various parameters: N—hardening exponent, T—transverse stress applied to the sample, D—elastic cell size.

$\Gamma_G/\sigma_Y\epsilon_Y = 10\,\mu$m. If the measured fracture energy $\Gamma_{SS} = 10\,\text{J/m}^2$, one finds from Fig. 5 that $D \approx 0.5\,\mu$m.

In an experiment with a single crystal of copper, diffusion bonded to a sapphire disc [7], interface debonding was driven in two crystallographic directions at slightly different energy release rates. The phenomenon was interpreted according to the Rice–Thompson model: dislocations emit from the crack tip in one direction but not from the other. An alternative interpretation appears to be possible on the basis of the present theory: both the crack tips do not emit dislocations; the different debond energies result from the different extent of background dislocation motion. Indeed, the micrographs show much denser slip lines in one case than the other. Experiments at higher magnifications are needed to ascertain which of the two interpretations is appropriate for the copper/sapphire system. Calculations within the framework of the present theory, taking into account of single crystal plasticity, are in progress to facilitiate a direct comparison with such experiments.

4. STRESS-ASSISTED CORROSION

In an ambient environment, the crack on a metal/ceramic interface can grow with a finite velocity under loads smaller than the failure load measured in an inert gas [5, 6]. Plasticity is present in both cases. The phenomenon can be understood in two steps: (1) a chemical reaction at the crack tip that weakens the atomic bond, and (2) load shielding by the background plasticity. The elastic cell provides the required high stress to partially separate the atomic planes, facilitating the transport of degrading species (e.g. water molecules). The bond-weakening reaction is diffusion-limited; the crack velocity depends on temperature and crack opening profile. The latter, in turn, is controlled by $\mathcal{G}_{tip}$. The growth law can be obtained by modeling a prescribed diffusion mechanism, or by direct measurement. A phenomenological growth law is

$$v = \begin{cases} v_0(\mathcal{G}_{tip}/\Gamma_G)^n & \text{for } \mathcal{G}_{tip} < \Gamma_G; \\ \infty & \text{for } \mathcal{G}_{tip} = \Gamma_G. \end{cases} \tag{2}$$

where v_0 and n are fitting parameters, and v_0 is temperature-dependent. Observe that $\mathcal{G}_{tip}$ is shielded by background plastic flow as described by (1). Combining (2) with Fig. 5 [or equation (1)], one obtains the crack velocity at a given remote load $\mathcal{G}$.

In the experiments on gold/sapphire interfaces [5], gold foils of various thickness, h, are sandwiched between sapphire plates. The plastic dissipation is limited by the foil thickness as governed by a dimensionless parameter $h\sigma_Y\epsilon_Y/\mathcal{G}_{tip}$. Once the growth law (2) and elastic cell size D are fitted with the data obtained from experiments with one thickness h, the response for other foil thickness can be predicted by computation. Combined experiments and computations could ascertain the validity of the present theory.

5. CRACK SPEED VS DISLOCATION MOBILITY

Consider a crack propagating at a velocity v in a cleavable, rate-sensitive metal; the crack tip is kept sharp in an elastic cell. The dislocation mobility is represented by continuum visco-plasticity. The plastic strain rate, $\dot{\epsilon}^P$, depends on the applied stress, σ, in accordance with

$$\dot{\epsilon}^P = \dot{\epsilon}_0 F(\sigma/\sigma_Y). \tag{3}$$

where σ_Y is the yield stress, and $\dot{\epsilon}_0$ a material constant related to dislocation mobility, both depending on the temperature.

The plastic shielding is still described by (1), but g now depends on two additional parameters, $\beta = (v\sigma_Y\epsilon_Y)/(\mathcal{G}_{tip}\dot{\epsilon}_0)$ and $m = v/c_R$, c_R being the Rayleigh wave speed. The first parameter measures crack speed in terms of dislocation mobility, and the second captures the effect of inertia. When D in (1) vanishes, the model in [16, 17] is recovered at high v/c_R. Unlike the previous model, the qualitative features of the present model do not rely on the details of the visco-plastic law, i.e. the functional form of F in (3). Moreover, the present theory treats slow and fast cleavage from a unified point of view. From this viewpoint the essential condition for cleavage is near-tip elasticity that keeps crack sharp. A new class of problems can be treated where dislocation mobility is so low that rate effects become pronounced even when $v/c_R \approx 0$. The shielding ratio $\mathcal{G}/\mathcal{G}_{tip}$ depends primarily on β: $\mathcal{G}/\mathcal{G}_{tip} = 1$ when $\beta = \infty$, and the quasi-static results in Fig. 5 are recovered when $\beta = 0$. Model computations of this type are in progress.

The ability of a cleavable, rate-sensitive metal to arrest a crack may be studied experimentally by using artificial elastic cells (Fig. 6). A step is created in a metal substrate and a layer of ceramic deposited. Two such substrates are then bonded with a well-defined

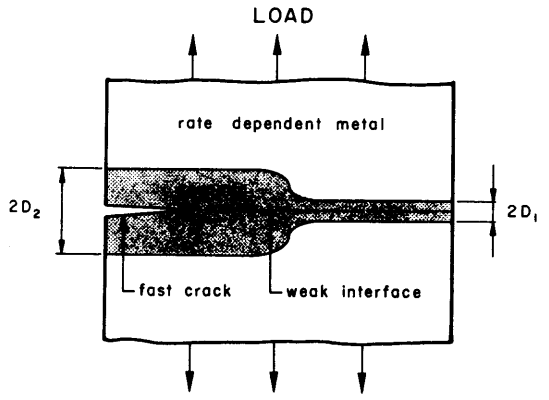

Fig. 6. A proposed experiment to demonstrate the ability of a metal to arrest a dynamically propagating crack.

interface. Thickness D_2 is large so that no background plasticity results in this region; the crack runs dynamically into the region with thickness D_1. Since D_1 controls the amount of plastic dissipation, the ability of the system to arrest the crack can be studied systematically by varying D_1.

6. STABLE CLEAVAGE CRACKING UNDER CYCLIC LOADING

A physical model for fatigue cracking must address the following questions: why crack grows stably at substantially lower load than the monotonic failure load, and how the growth per cycle depends on the loading magnitude. We focus on fatigue crack growth in cleavable, rate-independent materials, or along weak metal/ceramic interfaces. The remote loading, $\mathcal{G}$, alternates in the range $0 \leqslant \mathcal{G} \leqslant \mathcal{G}_{max}$. When $\mathcal{G}_{max} \leqslant \Gamma_G$, the plasticity does not provide any shielding so that $\mathcal{G}_{tip} \leqslant \Gamma_G$; the crack remains stationary and the background material undergoes cyclic plasticity. When $\mathcal{G}_{max} > \Gamma_G$, the crack grows and $\mathcal{G}_{tip} = \Gamma_G$ when $\mathcal{G} > \Gamma_G$. Non-proportional plasticity is induced in the process, so that the material no longer undergoes cyclic deformation. That is, the crack must grow under reloading to create new plastic zone to receive sufficient shielding. Within the framework of this theory the threshold toughness is Γ_G. Loading frequency effects can originate from either rate dependent plastic flow in the background, or diffusion-limited processes near the tip.

All the effects can be quantified once two sets of material properties are prescribed, one for the background plastic flow, and the other for the near-tip cohesion. For a cleavable, rate-independent material with Griffith energy Γ_G, yield stress σ_Y and yield strain ϵ_Y, using a model similar to that in Fig. 3, one can analyze the continuum problem under cyclic loading. Dimensional consideration dictates that

$$\frac{\lambda}{\Gamma_G/\epsilon_Y\sigma_Y} = \mathcal{F}\left(\frac{D\epsilon_Y\sigma_Y}{\Gamma_G}, \frac{\mathcal{G}_{max}}{\Gamma_G}\right) \tag{4}$$

where λ is crack growth per cycle. Detailed calculations would reveal whether this model could predict the widely observed Paris law.

Sorting out mechanisms in fatigue cracking has been difficult. Our theory suggests that the two elements key to fatigue cracking are near-tip bridges and background dissipation. They can be studied independently, for the same metal, by two experiments. In Fig. 7(a) the metal substrates contain a ceramic layer of micron thickness; the fracture energy of the ceramic has been measured independently. The thickness of the ceramic layer sets the extent of plastic dissipation in the metal substrates which can be determined in this experiment. Figure 7(b) describes an experiment designed to measure the fatigue properties of the near-tip bridges in the metal, background plasticity being absent.

7. SMALL CRACKS

An advantage for a mechanism-based theory is that it applies to small as well as large cracks. Consider a small penny-shaped crack in a cleavable, rate-independent material, subject to a remote, monotonically increasing, triaxial tension $\bar{\sigma}$. The conditions are representative of a small crack near the tip of a long, blunted crack. The small crack begins to grow with $\mathcal{G}_{tip} = \Gamma_G$ and a small plastic zone; larger plastic zones develop to shield the crack as it grows. Dimensional considerations suggest that

$$\frac{\bar{\sigma}}{\sigma_Y} = \Sigma\left(\frac{D\epsilon_Y\sigma_Y}{\Gamma_G}, \frac{a\epsilon_Y\sigma_Y}{\Gamma_G}, \frac{L}{a}\right) \tag{5}$$

where a is initial crack size, and L the crack extension. The critical stress for unstable crack growth,

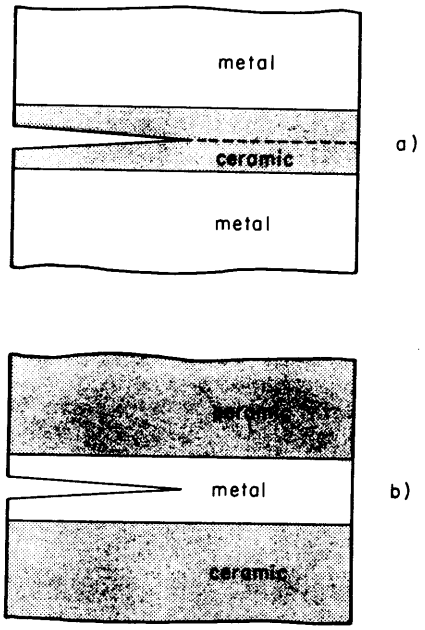

Fig. 7. A proposed experiment to sort out the roles of near-tip bridges and background plasticity on fatigue cracking.

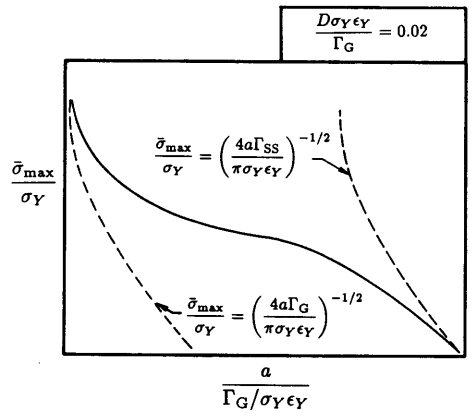

Fig. 8. The critical stress for unstable growth of a finite crack. The Griffith criterion applies for short and long cracks, with Γ_G and Γ_{SS}, respectively.

$\bar{\sigma}_{max}$, depends on materials and initial crack size. This dependence is illustrated in Fig. 8. The Griffith criterion may be used for both very short and very long cracks, with different fracture energies, Γ_G and Γ_{SS}. The critical stress for intermediate crack size should be obtained by analyzing the model system. Short cracks in transformation-toughened ceramics exhibit similar behaviors [23].

The problem becomes even more interesting when the background inelasticity is rate-dependent. When the small crack can outrun the background dislocation motion, the cleavage process continues with small amount of plasticity. By contrast, the same material containing a big crack may generate much larger plastic zones before it fractures. This happens in mild steels, where a big crack blunts, setting a high triaxial stress ahead of the tip which triggers a small crack to run dynamically to the big crack [14].

8. CONSTRAINT EFFECTS

Cleavage fracture is an issue of central importance for aging nuclear reactors. The measured toughness is found to depend on test geometries [24, 25], leading to a suggestion that fracture experiments be conducted using specimens comparable to pressure vessel wall thickness (about 9 inches) under biaxial loading. Because of the high cost, only a few such tests can be conducted for final validation. It has been demonstrated that data measured from different specimens under well-contained yielding can be correlated in terms of the T–stress [26, 27]. That is, toughness depends on T, represented by a toughness curve $J_c(T)$.

A more fundamental approach would be mechanism-based. From previous discussions it is clear that progress can be made by studying the effect of the T–stress on the near-tip bridges, and on background plasticity. Depending on temperatures and loading rates, near-tip bridges can be atomic cohesion, ductile tearing or hole growth. Studies on all three mechanisms are in progress [28]. Here we focus on the low-temperature cleavage. The presence of T does not affect the cleavage process, i.e. the value of Γ_G. However, T changes the plastic zone size. For example, a negative T generates large plastic zone at fixed Γ_G. This effect can be quantified by using the model system in Fig. 3, subjected to various values of T/σ_Y; finite element results are included in Fig. 5. Also observe that T–stress up to the yield stress, induced by thermal mismatch, is usually present near a metal/ceramic interface, which can be studied in a similar way.

9. MIXED-MODE FRACTURE ALONG METAL/CERAMIC INTERFACES

Metal/ceramic interfaces are convenient for studying cleavage with background plasticity [5–9, 29, 30]. The extent of plasticity can be varied by the ratio of shearing to opening stresses, σ_{xy}/σ_{yy}. Within the elastic cell, the standard elastic singular solution applies down to several Burgers vectors away from the crack tip. The elastic field can be characterized by a complex stress intensity factor, K_{tip}, written in the form [31]

$$K_{tip} = |K_{tip}| b^{-i\epsilon} \exp(i\psi_b). \tag{6}$$

Here $|K_{tip}|$ is the magnitude of the complex stress intensity factor, related to $\mathcal{G}_{tip}$ through an Irwin-type formula; ϵ is a small real number depending on the elastic constants of the metal and ceramic—$\tan\psi_b$ is representative of the ratio σ_{xy}/σ_{yy} immediately outside the decohesion core.

Remote loading can also be characterized in a similar way, i.e.

$$K = |K| L^{-i\epsilon} \exp(i\psi_L). \tag{7}$$

Here $|K|$ is related to the remote energy release rate, $\mathcal{G}$, by the same Irwin-type formula. The length L can be chosen to be of the order of the plastic zone size, so that $\tan\psi_L$ represents the ratio, σ_{xy}/σ_{yy}, just outside of the plastic zone. For a cleavable material, $\mathcal{G}_{tip} = \Gamma_G$, which may be insensitive to ψ_b, at least when the interface is loaded with a significant amount of tension. The plastic zone size depends on ψ_L, so is the measured fracture energy as represented by $\Gamma(\psi_L)$. Computations with a model system similar to Fig. 3 would predict $\Gamma(\psi_L)$; comparison with the experiments would ascertain the range of validity of the present theory.

10. CONCLUDING REMARKS

Several general conclusions can be drawn from the preceding discussions. Fracture process can be partitioned into near-tip bridging and background dissipation. This partitioning must be made at a length scale relevant to the dominant fracture mechanism. Atomic decohesion dominates when no dislocation emit from the crack tip and no other bridging mech-

anisms operates. Artificial layered materials are proposed as test geometries to sort out the roles played by near-tip bridges and background dissipation. More calculations are in progress [32]. Micron-scale fracture processes, such as hole growth and ductile tearing may also serve as bridges. In this regard, when several fracture mechanisms compete, the long range mechanism usually dominates. The implications of these models on dynamic fracture are being investigated [28].

Acknowledgements—We are grateful to Dr G. E. Beltz, Professor K. J. Hsia and many of our colleagues at Brown Univeristy for stimulating discussions. The work of Z. Suo was supported by NSF Young Investigator Award, by DARPA/URI Contract N00014-86-K-0753, and by a visiting Associate Professor appointment at Brown University funded by NRC/ONR Grant N00014-90-J1380. The work of C. F. Shih and A. G. Varias was supported by NRC/ONR Grant N00014-90-J13800, and by the Materials Research Group through Grant DMR-9002994.

REFERENCES

1. J. R. Rice, *J. Mech. Phys. Solids* **40,** 239 (1992).
2. H. C. Choi, A. F. Schwartzman and K.-S. Kim, in *Thin Films: Stress and Mechanical Properties*. Materials Research Society Proceedings (1992).
3. V. A. Lubarda, J. A. Blume and A. Needleman, *Acta metall. mater.* **41,** 625 (1993).
4. L. P. Kubin, G. Canova, M. Condat, B. Devincre, V. Pontikis and Y. Brećhet, submitted for publication.
5. I. E. Reimanis, B. J. Dalgleish and A. G. Evans, *Acta metall. mater.* **39,** 3133 (1991).
6. T. S. Oh, R. M. Cannon and R. O. Ritchie, *J. Am. Ceram. Soc.* **70,** C352 (1987).
7. G. E. Beltz and J.-S. Wang, *Acta metall. mater.* **40,** 1675 (1992).
8. N. P. O'Dowd, M. G. Stout and C. F. Shih, *Phil. Mag. A* **66,** 1037 (1992).
9. J. S. Wang and P. M. Anderson, *Acta metall. mater.* **39,** 779 (1991).
10. A. Needleman, *J. appl. Mech.* **54,** 525 (1987).
11. A. Needleman, *J. Mech. Phys. Solids* **38,** 289 (1990).
12. A. G. Varias, N. P. O'Dowd, R. J. Asaro and C. F. Shih, *Mater. Sci. Engng A* **126,** 65 (1990).
13. V. Tvergaard and J. W. Hutchinson, *J. Mech. Phys. Solids* **40,** 1377 (1992).
14. J. R. Rice and M. A. Johnson, in *Inelastic Behavior of Solids* (edited by M. F. Kanninen *et al.*), p. 641. McGraw-Hill, New York (1970).
15. R. O. Ritchie, J. F. Knott and J. R. Rice, *J. Mech. Phys. Solids* **21,** 395 (1973).
16. L. B. Freund and J. W. Hutchinson, *J. Mech. Phys. Solids* **33,** 169 (1985).
17. P. A. Mataga, L. B. Freund and J. W. Hutchinson *J. Phys. Chem. Solids* **48,** 985 (1987).
18. A. Argon, *Acta metall.* **35,** 185 (1987).
19. M. L. Jokl, V. Vitek and C. J. McMahon Jr, *Acta metall.* **28,** 1479 (1980).
20. J. R. Rice and J. S. Wang, *Mater. Sci. Engng A* **107,** 23 (1989).
21. R. M. McMeeking and A. G. Evans, *J. Am. Ceram. Soc.* **65,** 242 (1982).
22. B. Budiansky, J. W. Hutchinson and J. C. Lambropoulos, *Int. J. Solids Struct.* **19,** 337 (1983).
23. D. M. Stump and B. Budiansky, *Acta metall.* **37,** 3297 (1989).
24. E. M. Hackett, J. A. Joyce, R. H. Dodds Jr and C. Roe, *Elastic-Plastic Fracture Mechanics of Light Water Reactor Alloys*, FY 90 Annual Report, NUREG 0975, Vol. 8 (1990).
25. M. T. Kirk, K. C. Koppenhoefer and C. F. Shih, *ASTM-STP*, in press.
26. C. Betegón and J. W. Hancock, *J. appl. Mech.* **58,** 104 (1991).
27. N. P. O'Dowd and C. F. Shih, *J. Mech. Phys. Solids* **40,** 939 (1992).
28. K. J. Hsia, Z. Suo and C. F. Shih, work in progress.
29. A. G. Evans, M. Ruhle, B. J. Dalgleish and P. G. Charalambides, in *Metal/Ceramic Interfaces* (edited by M. Rühle, A. G. Evans, M. F. Ashby and J. P. Hirth), Vol. 4, p. 345. Pergamon Press, Oxford (1990).
30. R. M. Cannon, B. J. Dalgleish, R. H. Dauskardt, R. M. Risher, T. S. Oh and R. O. Ritchie, in *Fatigue of Advanced Materials* (edited by R. O. Ritchie, R. H. Dauskardt and B. N. Cox). MCEP Publishing, Edgbaston, U.K. (1991).
31. J. R. Rice, Z. Suo and J. S. Wang, in *Metal/Ceramic Interfaces* (edited by M. Rühle, A. G. Evans, M. F. Ashby and J. P. Hirth), Vol. 4, p. 269. Pergamon Press, Oxford (1990).
32. L. Xia, Z. Suo, C. F. Shih and A. G. Varias, work in progress.